Transmission Capacity of Carrier Sensing Ad Hoc Networks with Multiple Antennas

Andrew M. Hunter, Radha Krishna Ganti, and Jeffrey G. Andrews

***Abstract*—Multiple antennas have become a common component of wireless networks, improving range, throughput, and spatial reuse, both at the link and network levels. At the same time, carrier sensing is a widely used method of improving spatial reuse in distributed wireless networks, especially when there is limited coordination among non-communicating nodes. While the combination of carrier sensing and multiple antennas has been considered in the literature, physical layer spatial models and the attendant consequences have not been included. The primary reason for this has been the difficulty of analyzing functionals of interacting point processes. Having developed new methods of quantifying physical layer performance with robust spatial network models, we use these techniques to address the following questions: What multiple antenna techniques produce the best network performance, and what is the performance gain? And, how should multiple antennas interact with carrier sensing parameters? Overall, the analysis confirms the significant benefit of multiple antennas in distributed wireless networks.**

I. Introduction

As the number of wirelessly connected devices grows, so will the need for these devices to create flexible, decentralized networks. At the same time multiple antennas and carrier sensing-based medium access are two common performance enhancing features of modern wireless systems, even in energy- and cost-constrained systems. Theoretical studies of decentralized networks with carrier sensing have struggled with the analytical expressions for the interference of correlated point processes, difficulties which are only compounded by more complicated physical layers. In this paper we develop a model to link key carrier sensing parameters to environmental and network performance parameters in wireless ad hoc networks of nodes equipped with adaptive multi-antenna radios.

A few studies have approached the difficult problem of medium access control (MAC) analysis in random spatial field of interference including [1], [2], [3], and [4], while at the same time [5], [6], and [7] have considered multi-antenna (MIMO) radios, though they have focused mainly on the Aloha case. As a point of comparison, the study [5] developed a particular coordinated protocol as a comparison point against Aloha. The present work develops a new model for the combination of a multiple-antenna physical layer with a tunable CSMA model which includes Aloha as a special case. This allows the interaction of MIMO and CSMA to be studied and provides a framework for determining which MIMO configurations yield the highest gains for carrier-sensing networks as a whole, as well as enabling comparisons against Aloha.

The authors are with the Wireless Networking and Communications Group (WNCG) of the Electrical and Computer Engineering Department, The University of Texas at Austin, Austin, TX, 78712-0240 USA (email: {hunter, rganti, jandrews}@ece.utexas.edu).

II. System Model

For the underlying physical layer model, we consider a set of nodes, each having similar radios, randomly distributed on $\mathbb{R}^2$, communicating in a slotted system without any central controller. The nodes are assumed to be distributed as a spatial Poisson point process prior to the operation of any medium access mechanism. A path loss exponent of α characterizes large scale fading, while small scale fading is Rayleigh between any pair of antennas. The analysis will focus on a typical receiver located at the origin with its intended transmitter a distance R away.

At the physical layer, a transmission is assumed to be successful if the SINR is greater than some target threshold θ_{S}, where the SINR is given by the expression:

$$\mathrm{SINR} = \frac{S_o R^{\alpha}}{\sum_{j\in\Phi_t} S_j d_j^{-\alpha} + \frac{1}{\mathrm{SNR}}}, \tag{1}$$

where S_o is the fading signal level at the detection point, and S_j and d_j are the fading interference level and distance to the jth interferer, respectively, and Φ_t is the point process of actively interfering nodes around a typical receiver. Given that θ_{S} is met over a slot, the achievable rate will be $\log_2(1+\theta_{\mathrm{S}})$.

A. Performance Metrics

Ultimately, the principal design goal is to maximize network sum throughput, or equivalently, area spectral efficiency. However, recognizing that physical layer implementation and user experience cannot abide degenerate cases, two types of quality requirements are introduced. First, as mentioned above, a target SINR θ_S is required on any particular attempted transmission, which results in an outage if not met. Second, the outage probability ϵ can also be taken as a constraint on any given link or transmission. Transmission capacity is defined as the mean density of *successful* transmissions that can occur with given quality constraints (i.e., θ_{S}, and ϵ are satisfied). Given the success probability function $\mathbf{P}_{\mathrm{S}}(\lambda_t)$, the transmission capacity is

$$\mathrm{TC} = \arg\max_{\lambda_t} \lambda_t \cdot \mathbf{P}_{\mathrm{S}}(\lambda_t). \tag{2}$$

Lastly, area spectral efficiency is the transmission capacity scaled by the data rate achieved in each of those transmissions: $M_t \log_2(1+\theta_{\mathrm{S}})\lambda_t \cdot \mathbf{P}_{\mathrm{S}}(\lambda_t)$, where M_t is the number of data

streams transmitted on each link. For simplicity of presentation, when multiple antennas are used at the transmitter for spatial multiplexing we assume two things: first, each spatial mode will treated as a separate transmission, carrying a separate packet and decoded separately. Second, the same outage constraint will be applied across all modes of all links independently. More elaborate arrangements of modes and outages can be devised and analyzed, but these necessarily lead to more cumbersome expressions best considered outside the space here.

B. The MIMO Channel

Each transmitter has N_t and each receiver has N_r antennas to decode $M_t \leq \min\{N_t, N_r\}$ independent transmitted data streams. In Rayleigh fading, the channel between the receiver of interest and its intended transmitter is $R^{-\frac{\alpha}{2}}\mathbf{H}$ which is an $N_t \times N_r$ matrix of i.i.d. complex Gaussian entries with unit variance scaled by a power-law path loss factor. This channel can be decomposed into spatial modes by means of its SVD when channel state information (CSI) is available at the transmitter, while in the absence of transmitter CSI, the receiver can decode equal power and rate streams by various techniques including zero-forcing (ZF) or maximal-ratio-combining [5]. The ZF beamforming solution for a receiver with CSI is the pseudo-inverse: $(\mathbf{H}^H\mathbf{H})^{-1}\mathbf{H}^H$, where $\cdot^H$ denotes the Hermitian transpose.

The results here will be restricted to the case of open-loop zero-forcing multiplexing methods. A number of other techniques with and without CSI at the transmitter follow very similar expressions, but this provides a rich enough set of options to demonstrate the relationships between CSMA and MIMO techniques.

C. "Soft" Carrier Sensing

We consider a "soft" CSMA model which takes into account two effects:

1) Large-scale density λ_t of transmitters.
2) Shot range inhibition.

Large-scale density : We use a Matern model similar to [1] for obtaining the final density of transmitters. In this model each node is associated with a set $\hat{\mathcal{N}}$ consisting of transmitters which individually cause an interference greater than θ_{M}. A node is finally selected to transmit if its timer (a uniform random variable in $[0, 1]$) is the smallest. Given an initial density λ_i of nodes attempting to access the channel, after carrier sensing the resulting large-scale density λ_t is [1]

$$\lambda_t = \lambda_i \cdot \frac{1 - \exp(-\mathcal{N})}{\mathcal{N}}, \tag{3}$$

where $\mathcal{N}$ is the average number of nodes in a typical contention set $\hat{\mathcal{N}}$ and equals

$$\begin{aligned} \mathcal{N} &= \int_{\mathbb{R}^2} \lambda_i \cdot e^{-\theta_{\mathrm{M}}|x|^\alpha} \mathrm{d}x, \\ &= \pi\Gamma(1 + 2/\alpha)\theta_{\mathrm{M}}^{-2/\alpha}\lambda_i. \end{aligned} \tag{4}$$

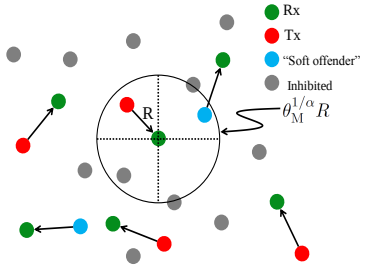

Fig. 1. Contention around the typical receiver. Fading and channel sensing errors lead to a "soft" CSMA model unlike the corresponding hard care boundary marked here.

Shot range inhibition: We make a further approximation that from the perspective of a typical receiver, the set of interferers is distributed around it as a radially symmetric inhomogeneous Poisson process with density $(1-e^{-\theta_{\mathrm{M}}|X|^\alpha})\lambda_t$, where λ_t is the average density of the set of currently transmitting nodes. $e^{-\theta_{\mathrm{M}}|X|^\alpha}$ is the probability that an exponentially distributed power fade will exceed a threshold θ_{M} at that distance. The average density is all that is necessary to model the interference contribution from nodes at long distances, while at close ranges the presence of the communicating node has the dominant effect on the distribution of interferers. Furthermore, the model treats the channel through which carrier sensing decisions were made as independent of the Poisson shot noise interference process of data transmission. In this sense the carrier sensing is "soft," being neither an exact geographic disk, nor exactly representative of mutually interfering nodes during data communication.

Final model: From the perspective of a typical receiver the interferers form a non-homogeneous Poisson point process of density $(1-e^{-\theta_{\mathrm{M}}|X|^\alpha})\lambda_t$. This model has several advantages over the hard-core model: First, it brings fading into play when modeling carrier sensing. Second, it allows for modeling imperfect carrier sensing. Third, it enables modeling of a behavior specific to multi-antenna systems in which network interference differs between the control/carrier sensing modes and high data rate modes. Lastly, it provides more tractable results that give simpler functional relationships between the carrier sensing parameters and other environmental and system parameters. In addition, a model in which the probability of inhibition rises at least as fast as the power-law path loss function results in the interference power from the nearest interferer having finite mean. This removes problems related to the behavior of the path loss model near the origin (a feature shared by the Matern hard-core model).

D. CSMA Sensing with Multiple Antennas

Another way a CSMA ad hoc network can take advantage of multiple antennas is in the carrier sensing itself. When the carrier sensing mechanism is subject to fading, more conservative thresholds must be met to guarantee outage requirements. One approach which is readily tractable in the current model is to use selection or combining diversity on

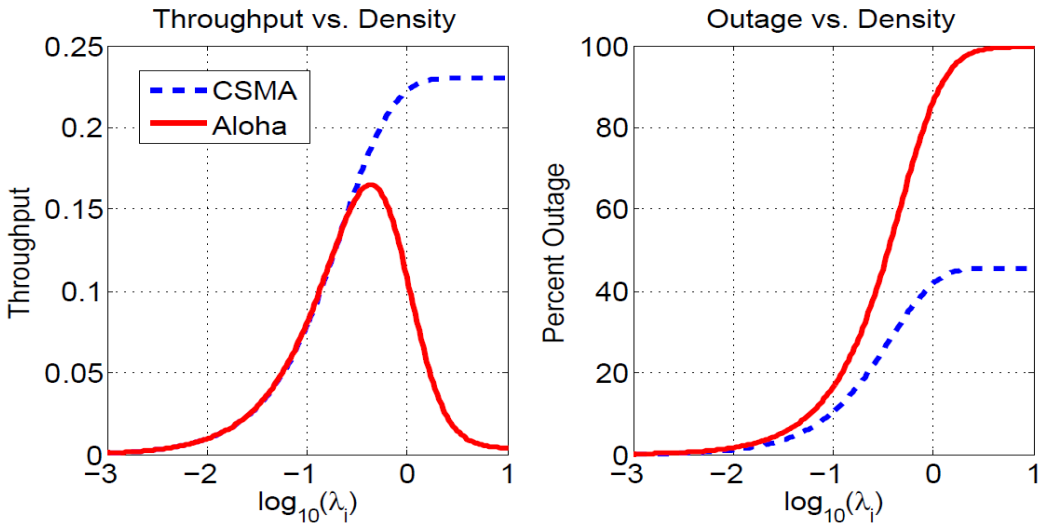

Fig. 2. Comparison of throughput and outage for CSMA and Aloha, for SISO system. Density is *initial* density, i.e., before thinng via carrier sensing. Outage is counted among active transmitters (i.e., those not thinned by CSMA). Parameters were $R = 1, \alpha = 4, \theta_{\rm S} = 0$dB.

multiple receive antennas for carrier sensing and to impose a threshold on the selected or combined output (the former approach being appropriate when CSI over the control channel is difficult to obtain). As an example, suppose a node with M_c multiple receive antennas performs carrier sensing on each antenna, but averages the results across antennas before applying the threshold. In this case

$$\begin{aligned}\mathcal{N} &= \int_{\mathbb{R}2} \lambda_i \cdot e^{-\theta_{\rm M} M_c |x|^\alpha} \sum_{k=0}^{M_c-1} \frac{(\theta_{\rm M} M_c |x|^\alpha)^k}{k!} {\rm d}x \\ &= \frac{2\pi}{\alpha} \theta_{\rm M}^{-\frac{2}{\alpha}} \lambda_i \sum_{k=0}^{M_c-1} \frac{\Gamma(\frac{2}{\alpha}+k)}{M_c^{\frac{2}{\alpha}} \Gamma(k+1)}. \end{aligned} \quad (5)$$

Note that in the limit of a large number of antennas, the carrier sensing behavior approaches that of a hard-core process as the influence of small scale fading on sensing decisions disappears. While channel hardening techniques make the carrier sensing mechanism more efficient, primarily by reducing errors due to deep fades, the net benefit turns out to be small (in particular small compared to the benefit of CSMA over Aloha). Therefore, for the main analysis of multiplexing systems, a SISO carrier sensing channel is assumed.

III. Open-Loop Spatial Multiplexing with CSMA

We now state the central result of the paper which deals with the probability of success or equivalently the SINR distribution.

Theorem 1: Given a network of nodes performing CSMA, open-loop spatial multiplexing, and with per-stream decoding success defined in (1),

$$\mathbf{P}_{\rm S}(\theta_{\rm S}) = \sum_{k=0}^{N_r-1} \left[\frac{(-s)^k}{k!} \frac{{\rm d}^k}{{\rm d}s^k} \mathcal{L}_{I_\Phi}(s) e^{-\frac{1}{\rm SNR}}(s) \right]_{s=N_t \theta_{\rm S} R^\alpha},$$

where

$$\mathcal{L}_{I_\Phi}(s) = \exp\left\{ -\frac{2\pi}{\alpha} (s/N_t)^{\frac{2}{\alpha}} \lambda_t [C_{N_t}^\alpha - T_{\rm M}(s)] \right\}$$

$$C_{N_t}^\alpha = \sum_{i=1}^{N_t} \binom{N_t}{i} B(N_t - i_\alpha, i_\alpha)$$

$$T_{\rm M}(s) = \sum_{i=1}^{N_t} \binom{N_t}{i} \Gamma(N_t - i_\alpha) U\left(N_t - i_\alpha, 1 - i_\alpha, \frac{\theta_{\rm M}}{N_t} s\right)$$

with $i_\alpha = i - 2/\alpha$ for notational convenience and $B(x,y) = \frac{\Gamma(x)\Gamma(y)}{\Gamma(x+y)}$ being the beta function, and where $U(a,b,x) = \frac{1}{\Gamma(a)} \int_0^\infty e^{-xt} t^{a-1} (1+t)^{b-a+1} {\rm d}t$ is Kummer's confluent hypergeometric U-function.

Proof: See the appendix, which develops these expressions using techniques similar to those of [1] and [6]. In addition the appendix derives an efficient method of evaluating the derivatives both symbolically and numerically. ■

Again we note that as $s \to \infty$, $U(a,b,s) \to 0$ and thus $T_{\rm M} \to 0$ which corresponds to the Aloha case. As $s \to 0$, $\Gamma(a)U(a,b,s) \to B(a,b)$, which implies that $T_{\rm M} \to C_{N_t}^\alpha$ as the threshold $\theta_{\rm M} \to 0$. In this case the probability of success approaches 1 among active transmitters, at the expense of λ_t vanishing.

A. Optimal CSMA threshold

Specializing Theorem 1 to the case $N_r = N_t = 1$, we obtain the success probability in a SISO system as

$$\mathbf{P}_{\rm S}(\theta_{\rm S}) = \exp\left\{ -\theta_{\rm S}^{2/\alpha} R^2 \lambda_t \left[C(\alpha) - T_{\rm M} \right] \right\} e^{-\theta_{\rm S} R^\alpha / {\rm SNR}},$$

where $C(\alpha) = \pi\Gamma(1+2/\alpha)\Gamma(1-2/\alpha)$ is the familiar Aloha constant and

$$T_{\rm M} = \frac{2\pi}{\alpha} e^{\theta_{\rm M}\theta_{\rm S} R^\alpha} \Gamma\left(1 - \frac{2}{\alpha}, \theta_{\rm M}\theta_{\rm S} R^\alpha\right) \quad (6)$$

the two-parameter gamma function being the upper incomplete gamma function. Note that $T_{\rm M}$ is a factor related to the carrier sensing threshold, but also that λ_t is dependent on this threshold. This expression holds for any outage level or transmitter density. As the inhibition threshold rises so that very few nodes are inhibited, $\lambda_t \to \lambda_i$ and $T_{\rm M} \to 0$ recovering the Aloha result [1]. Note also that with a fixed threshold

$$\lim_{\lambda_i \to \infty} \lambda_{t,\infty} = \left(\pi \Gamma(1+2/\alpha)\theta_{\rm M}^{-2/\alpha}\right)^{-1}, \qquad (7)$$

which indicates that regardless of the number of users requesting access, the carrier sensing process limits the set of active transmitters to a limiting density, as it should.

A natural question then is to find the optimal carrier sensing threshold. The optimum threshold is then the unique maximum to:

$$\theta_{\rm M}^* = \arg\max_{\theta_{\rm M}} \lambda_t \cdot \exp\left\{-\theta_{\rm S}^{2/\alpha} R^2 \lambda_t \left[C(\alpha) - T_{\rm M}\right]\right\}. \qquad (8)$$

This expression is log-concave in $\theta_{\rm M}$ and hence is relatively easy to optimize numerically. At this point there are a few observations that can be made to assist further analysis: First, as $\lambda_i \to \infty$ the optimum threshold approaches a limit which is the unique solution to 8 at $\lambda_{t,\infty}$. Second, as λ_i becomes small, for a fixed threshold, very little inhibition takes place and the sum throughput performance of Aloha and CSMA are nearly identical[1] so that there is very little difference in an optimum versus a non-optimum threshold. Hence, a useful approximation is to consider the optimum threshold for any initial density to be roughly equal to that for the limiting density $\lambda_{t,\infty}$.

Lastly, as $\lambda_i \to 0$, the network is sparse enough that very little inhibition takes place and $\lambda_t \to \lambda_i$, and the spatial density of transmissions can be related to the outage probability:

$$\lambda_t = \frac{\epsilon}{\theta_{\rm S}^{2/\alpha} R^2} \cdot \frac{1}{\left[C(\alpha) - T_{\rm M}\right]} + o(\epsilon^2). \qquad (9)$$

The factor $T_{\rm M}$ is always less than or equal to $C(\alpha)$, and hence carrier sensing with an appropriate threshold represents a strict improvement over Aloha. For the multiple antenna case, the optimum $\theta_{\rm M}$ can be found numerically. As in the single-antenna case, the optimum threshold reaches a limit as λ_i grows large, which is a relatively good selection at all.

IV. Examples and Discussion

Fig. 2 compares throughput and outage of CSMA and Aloha for the base SISO case. Here the CSMA is not fully optimized, but rather has a fixed threshold for all initial contention densities. Note that the figures plot throughput and outage versus the initial contention density, prior to thinning via carrier sensing, in order for the comparison with Aloha to be fair, and this convention was used for all plots in the paper.

[1]This is very different from saying that the transmission capacity at a fixed outage is nearly the same for both. At a fixed λ_i, if Aloha experiences 1% outage, then CSMA can increase throughput at the same λ_i by no more than 1% at best. On the other hand, for a fixed 1% outage constraint, CSMA can maintain a substantially greater λ_t than Aloha can.

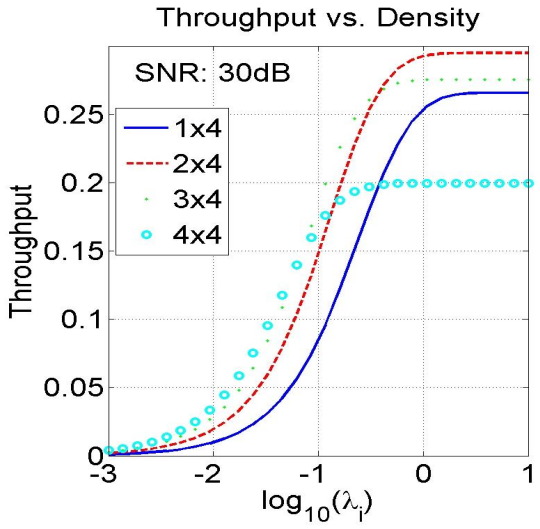

Fig. 3. Comparison of throughput for CSMA at a high base SNR. Note that no outage constraints are imposed. Parameters were $R = 1, \alpha = 4, \theta_{\rm S} = 0$dB.

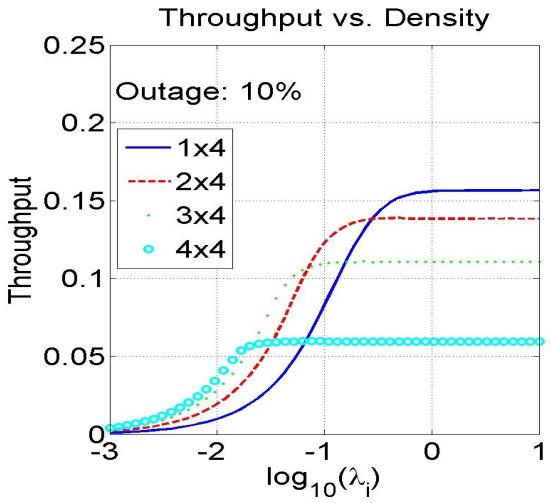

Fig. 4. Throughput vs. initial density for 4-antenna systems with optimized CSMA and an outage constraint of 10% Parameters were $R = 1, \alpha = 4, \theta_{\rm S} = 0$dB, SNR= 10dB.

Fig. 3 compares 4-antenna MIMO configurations at a high base SNR (with fully optimized CSMA). Fig. 4 compares 4-antenna MIMO configurations with a relatively small outage constraint applied. These curves demonstrate several distinctions between the performance of CSMA networks versus Aloha networks. The first is simply that as the initial contention density increases, CSMA throughput overtakes Aloha substantially and reaches a non-zero plateau. Furthermore, comparing throughput levels for Fig. 2 and Fig. 4, it becomes clear that CSMA MIMO systems achieve a higher throughput at substantially lower outage among transmitting nodes. This can substantially reduce the burden on PHY layer decoding implementations and conserve energy. In particular, note that a 1×3 antenna configuration with an optimized threshold can

achieve a network throughput equivalent to the best Aloha configuration but with a fourfold reduction in the outage probability.

V. Conclusion

This paper developed a model for CSMA and its interaction with multiple antennas in ad hoc wireless networks. The results confirm the benefit of CSMA and MIMO techniques in ad hoc networks, alone or in tandem. First, the throughput at any contention density is superior for optimized CSMA systems over their Aloha counterparts. Second, the carrier sensing mechanism results in a throughput plateau which is maintained with fixed operting parameters, unlike Aloha, even as network access requests increase. Third, CSMA systems achieve a higher throughput at substantially lower outage among transmitting nodes. And lastly, CSMA improves the environment for spatial multiplexing, in certain cases making a higher number of data streams more attractive at any spatial traffic density.

Appendix

For a given stream at the receiver using the ZF solution $S_o \sim \text{Gamma}(N_r, 1/N_t)$ with $F^c_{S_o}(x) = e^{-N_t x}\sum_{k=0}^{N_r-1}\frac{(N_t x)^k}{k!}$ so that

$$\begin{aligned}\mathbf{P}_{\text{S}}(\theta_{\text{S}}) &= \mathbf{P}\left(\frac{S_o R^{-\alpha}}{\sum_{i\in\Phi} S_i d_i^{-\alpha} + \frac{1}{\text{SNR}}} > \theta_{\text{S}}\right)\\ &= \int_0^\infty F^c_{S_o}(\theta_{\text{S}} R^\alpha t) f_{I_\Phi + \frac{1}{\text{SNR}}}(t)\text{d}t\\ &= \sum_{k=0}^{N_r-1}\frac{1}{k!}\int_0^\infty (st)^k e^{-s\cdot t} f_{I_\Phi+\frac{1}{\text{SNR}}}(t)\text{d}t\\ &= \sum_{k=0}^{N_r-1}\left[\frac{(-s)^k}{k!}\frac{\text{d}^k}{\text{d}s^k}\mathcal{L}_{I_\Phi}(s)\mathcal{L}_{\frac{1}{\text{SNR}}}(s)\right]_{s=N_t\theta_{\text{S}}R^\alpha},\end{aligned}$$

where the Laplace transform of the sum of the random variables is the product of the transforms. Now $\mathcal{L}_{\frac{1}{\text{SNR}}}(s) = e^{-s/\text{SNR}}$ and if in addition $S_i \sim \text{Gamma}(N_t, 1/N_t)$ as in open-loop multiplexing across the network, the Laplace transform of the Poisson shot noise is

$$\begin{aligned}\mathcal{L}_{I_\Phi}(s) &= \exp\left\{\int_{\mathbb{R}^2}\left(\text{E}_{S_i}\left[e^{-S_i|x|^{-\alpha}s}\right]-1\right)\text{d}\Phi\right\}\\ &= \exp\left\{-2\pi\lambda_t\int_0^\infty u\left(1-\frac{1}{(1+s/N_t u^\alpha)^{N_t}}\right)\right.\\ &\left.\times(1-e^{-\theta_{\text{M}}u^\alpha})\text{d}u\right\}\\ &= \exp\left\{-\frac{2\pi}{\alpha}\theta_{\text{S}}^{\frac{2}{\alpha}}R^2\lambda_t\sum_{i=1}^{N_t}\binom{N_t}{i}[B(N_t-i_\alpha,i_\alpha)-\right.\\ &\left.\Gamma(N_t-i_\alpha)U(N_t-i_\alpha,1-i_\alpha,\theta_{\text{M}}\theta_{\text{S}}R^\alpha)]\right\}\\ &= \exp\left\{-\frac{2\pi}{\alpha}\theta_{\text{S}}^{\frac{2}{\alpha}}R^2\lambda_t[C^\alpha_{N_t}-T_{\text{M}}]\right\}.\end{aligned}$$

Our last task is to find an explicit and efficient method of calculating derivatives of these Laplace transforms. For this we turn to Faà di Bruno's formula for derivatives of composite functions $\frac{\text{d}^k}{\text{d}s^k}f(g(s))$, which can be represented as a determinant [8]:

$$\frac{\text{d}^k}{\text{d}s^k}f(g(s)) = \det\mathbf{M}\, f(g(s))$$

for the $k\times k$ matrix

$$\mathbf{M} = \begin{pmatrix} g^{(1)}D & -1 & 0 & 0 & \dots\\ g^{(2)}D & g^{(1)}D & -1 & 0 & \dots\\ g^{(3)}D & 2g^{(2)}D & g^{(1)}D & -1 & \dots\\ g^{(4)}D & 3g^{(3)}D & 3g^{(2)}D & g^{(1)}D & \dots\\ \vdots & \vdots & \vdots & \vdots & \end{pmatrix},$$

where $D^k f(g(s)) = f^{(k)}(g(s))$, and where the coefficients applied to each row are rows of Pascal's triangle. To apply Faà di Bruno's formula to the derivatives of $\mathcal{L}_{I_\Phi}(s)\mathcal{L}_{\frac{1}{\text{SNR}}}(s)$, we can write $\mathcal{L}_{I_\Phi}(s)\mathcal{L}_{\frac{1}{\text{SNR}}}(s) = f(g(s))$, where $f(s) = e^s$ and $g(s) = \log\left(\mathcal{L}_{I_\Phi}(s)\mathcal{L}_{\frac{1}{\text{SNR}}}(s)\right)$ whose derivatives are (for $k>1$):

$$\begin{aligned}g^{(k)}(s) = -\frac{2\pi}{\alpha}\lambda_t(s/N_t)^{\frac{2}{\alpha}-k}\left[C^\alpha_{N_t}\prod_{j=0}^{k-1}\left(\frac{2}{\alpha}-j\right)-\right.\\ \left.\sum_{i=1}^{N_t}\sum_{j=0}^{k}K_{ijk}s^j U\left(\begin{bmatrix}N_t-i_\alpha+j\\ 1-i_\alpha+j\end{bmatrix},\frac{\theta_{\text{M}}}{N_t}s\right)\right],\end{aligned}\tag{10}$$

where

$$\begin{aligned}K_{ijk} = (-\theta_{\text{M}}/N_t)^j\binom{N_t}{i}\Gamma(N_t-i_\alpha)\binom{k}{j}(N_t-i_\alpha+j)_j\\ \prod_{n=0}^{k-j-1}\left(\frac{2}{\alpha}-n\right).\end{aligned}$$

To accomplish this we needed the relation for the nth derivative of $U(a,b,x)$ which is easily expressible as $\frac{\text{d}^n}{\text{d}x^n}U(a,b,x) = (-1)^n(a)_n U(a+n,b+n,x)$ where $(\cdot)_n$ is the Pochhammer symbol for the rising factorial.

References

[1] F. Baccelli, B. Blaszczyszyn, and P. Muhlethaler, "An ALOHA protocol for multihop mobile wireless networks," *IEEE Trans. on Inf. Theory*, vol. 52, no. 2, pp. 421–436, Feb. 2006.

[2] A. Hasan and J. G. Andrews, "The guard zone in wireless ad hoc networks," *IEEE Trans. on Wireless Comm.*, vol. 6, no. 3, pp. 897 – 906, Mar. 2007.

[3] M. Kaynia, G. Oien, and N. Jindal, "Impact of fading on the performance of ALOHA and CSMA," in *Proc., IEEE Signal Proc. Adv. in Wireless Comm. (SPAWC)*, Italy, Jun. 2009.

[4] R. K. Ganti and J. G. Andrews, "A new method for computing the transmission capacity of non-Poisson wireless networks," in *Proc., IEEE Intl. Symposium on Information Theory*, Austin, TX, 2010.

[5] R. H. Y. Louie, M. R. McKay, and I. B. Collings, "Open-loop spatial multiplexing and diversity communication in ad hoc networks," *available at arXiv:1009.3090v2*, Sep. 2010.

[6] A. M. Hunter, J. G. Andrews, and S. Weber, "Transmission capacity of wireless ad hoc networks with spatial diversity," *IEEE Trans. on Wireless Comm.*, vol. 7, no. 12, Dec. 2008.

[7] A. M. Hunter and J. G. Andrews, "Adaptive rate control over multiple spatial channels in ad hoc networks," in *Proc., Workshop on Spatial Stoch. Models for Wireless Net. (SpaSWiN)*, Berlin, Germany, Apr. 2008.

[8] W. P. Johnson, "The curious history of Faà di Bruno's formula," in *Amer. Math. Monthly*, vol. 109, no. 3, 2002.